JJMIE

Volume 5, Number 5, Oct. 2011
ISSN 1995-6665
Pages 461 - 470

Jordan Journal of Mechanical and Industrial Engineering

Modeling of Weld Bead Geometry and Shape Relationships in Submerged Arc Welding using Developed Fluxes

Vinod Kumar*,[a]

[a]*College of Engineering, Punjabi University, Patiala, India*

Abstract

To automate a welding process, which is the present trend in fabrication industry, it is essential that mathematical models have to be developed to relate the process variables to the weld bead parameters. Submerged arc welding (SAW) is characterized by its high reliability, deep penetration, smooth finish and high productivity especially for welding of pipes and boiler joints. In the present work mathematical models have been developed for SAW using developed fluxes. Response surface methodology has been used to predict critical dimensions of the weld bead geometry and shape relationships. The models developed have been checked for their adequacy and significance by using the F-test and the t-test, respectively. Main and interaction effects of the process variables on bead geometry and shape factors are presented in graphical form and using which not only the prediction of important weld bead dimensions and shape relationships but also controlling the weld bead quality by selecting appropriate process parameter values are possible.

Keywords: Weld bead geometry; RSM; Design of Experiment

1. Introduction

Quality has now become an important issue in today's manufacturing world. Whenever a product is capable of conforming to desirable characteristics that suit its area of application, it is termed as high quality. Therefore, every manufacturing process has to be designed in such a way that the outcome would result in a high quality product. The present trend in the fabrication industries is the use of automated welding processes to obtain high production rates and high precision. To automate a welding process it is essential to establish the relationship between process parameters and weld bead geometry to predict and control weld bead quality [1]. Submerged arc welding (SAW) is preferred over other methods of welding of pipes and boilers because of its inherent qualities like easy control of process variables, high quality, deep penetration, smooth finish, capability to weld thicker sections and prevention of atmospheric contamination of weld pool [2]. With the growing emphasis on the use of automated welding systems, SAW is employed in semiautomatic or automatic mode in industry [3]. In such automated applications, a precise means of selection of the process variables and control of weld bead shape has become essential because mechanical strength of welds is influenced not only by the composition of the metal, but also by the weld bead shape [2, 3].

The weld bead shape is an indication of bead geometry. The acceptable or appropriate weld bead shape depends on factors such as line power which is the heat energy supplied by the arc to the base plate per unit length of weld, welding speed, joint preparation, etc. Hence, study and control of weld bead shape is very much essential. To do this precise relationship between the process parameters and the bead parameters controlling the bead shape is to be established. This may be achieved by the development of mathematical expressions, which can be fed into a computer relating the weld bead dimensions to the important process control variables affecting these dimensions. Also, optimization of the process parameters to control and obtain the required shape and quality of weld beads is possible with these expressions.

In submerged arc welding approximately 10% -15% of the flux gets converted into very fine particles termed as flux dust before and after welding, due to transportation and handling. If welding is performed without removing these very fine particles from the flux, the gases generated during welding are not able to escape, thus it may result into surface pitting (pocking) and even porosity. On the other hand, if these fine particles are removed by sieving, the cost of welding will be increased significantly. And if this flux dust is dumped/ thrown, will create the pollution. Therefore to reduce the cost of welding and pollution, agglomerated fluxes have been developed [4] by utilizing wasted flux dust. The performance of the weldment obtained by using developed fluxes was checked by chemical analysis, radiography, mechanical and metallurgical tests; they showed good agreement with that of dictated by AWS for a perfect weld.

In the present study an attempt has been made to investigate the effect of using developed fluxes on different bead geometry parameters, including weld penetration shape factor, weld reinforcement form factor, through experiments based on design matrix. The analysis of variables (ANOVA) technique has been adopted to check the level and degree of the direct or interactive

* Corresponding author. e-mail: vk_verma5@rediffmail.com

effect of welding current, voltage, welding speed and flux basicity index on features of bead geometry and shape relationship. Response surface methodology has been applied to derive mathematical models that correspond to the welding phenomena using developed fluxes. Predictive equations have been used to represent graphically the effects of process parameters on various responses. No work so far has been performed which considers the four important process parameter used in this study using fluxes developed from waste flux dust.

2. Experimentation

The research work was planned to be carried out in the following steps [5]

- Selection of the important process control variables and finding their upper and lower limits
- Developing the design matrix
- Conducting the experiments as per the design matrix;
- Recording the response parameters
- Checking the significance of models and arriving at the final models
- Validation of models
- Presenting the direct and interaction effects of process parameters on bead geometry in graphical form
- Analysis of results.

2.1. Selection of process parameters and their working ranges:

Based on the effect on weld bead geometry, ease of control and capability of being maintained at the desired level, four independently controllable process parameters were identified namely, the open circuit voltage (A), current (B), welding speed (C) and Basicity Index (D). Trial runs were conducted by varying one of the process parameters at a time while keeping the rest of them at constant value [6]. The working range was fixed by inspecting the bead for a smooth appearance and the absence of visible defects. The upper and lower limits were coded as +1 and −1, respectively. The selected process parameters and their upper and lower limits together with notations and units are given in Table 1.

Table 1: Process control variables and their limits.

Parameters	Notations	Limits		
		-1	0	1
Voltage (volts)	A	32	35	38
Current (amperes)	B	375	425	475
Welding Speed (m/hr)	C	24	27	30
Basicity Index	D	0.6	0.9	1.2

2.2. Developing the design matrix:

Design of experiments is a powerful analysis tool analyzing the influence of process variables over some specific variable, which is unknown function of these process variables. It is the process of planning the experiments that appropriate data can be analyzed by statistical methods, resulting in valid and objective conclusions. Statistical approval to experiment design is necessary if we wish to draw meaningful conclusions from the data [7].

In submerged arc welding, process parameters interact in a complicated manner that influences various features of quality characteristics of the weld bead. Quadratic response surface methodology is an efficient approach to represent these relationships through mathematical equations, [7]. The graphical representations of these equations serve as means for investigating main/direct as well as interaction effects of various process parameters on selected response(s). Application of this technique can be found in the reporting of [8-9]. The RSM was employed to quantify the relationship between the individual response factors and the input machining parameters of the following form:

$$Y = F(A, B, C, D) \quad (1)$$

Where, Y is the desired response and F is the response function or response surface. The approximation of Y has been proposed by fitting second-order polynomial regression model i.e. quadratic model [10] of the following form:

$$Y = a_o + \sum_{i=1}^{i=4} a_i x_i + \sum_{i=1}^{i=4} a_{ii} x_i^{\,2} + \sum_{i<j}^{i=4} a_i x_i x_j \quad (2)$$

where, a0 is constant and ai, aii and aij respectively represent the coefficients of linear, quadratic and cross product terms. The xi reveals the coded variables corresponding to the studied welding parameters. The coded variables xi (1, 2, 3, and 4) are obtained from the following transformation equation:

$$x_1 = \frac{(A - A_o)}{\Delta A}, x_2 = \frac{(B - B_o)}{\Delta B}, x_3 = \frac{(C - C_o)}{\Delta C}, x_4 = \frac{(D - D_o)}{\Delta D}, \quad (3)$$

Where x_1,x_2,x_3 and x_4 are the coded values of input parameters A, B, C and D respectively and A0, B0, C0 and Do are the values of corresponding parameters at zero level. The terms ΔA, ΔB, ΔC and ΔD are the intervals of variation in A, B, C and D respectively.

The necessary data required for developing the response models have been collected by designing the experiments based on Box-Behnken Design (BBD) using state ease 6.0 version of design of experiment and by varying each numeric factor over three levels coded as -1, 0, and +1. The BBDs are available for 3 to 10 factors, which are formed by combining two-level factorial designs with incomplete block designs. This procedure creates designs with desirable statistical properties and more importantly, only a fraction of experiments are required, as compared to three-level factorial design [11-12]. The levels of four process parameters and experimental results are reported in Table 2. The values selected are well supported by earlier reported works.

Table 2: Design values and observed values of bead parameters.

Expt. Run No.	Process Parameters				Response factors				
	A Voltage (volts)	B Current (amperes)	C Welding Speed (m/hr)	D Basicity Index	W Bead Width (mm)	P Penetration (mm)	R Reinforcement (mm)	WPSF	WRFF
1	1	-1	0	1	17.76	6.545	3.201	2.71352	5.54827
2	-1	0	0	0	17.24	7.349	4.043	2.3459	4.26416
3	0	0	0	1	17.81	6.735	3.345	2.64439	5.32436
4	0	-1	1	1	15.192	6.671	2.955	2.27732	5.14112
5	-1	0	0	-1	16.79	10.455	6.025	1.60593	2.78672
6	0	-1	0	0	17.48	6.389	2.382	2.73595	7.33837
7	0	0	0	1	17.2	6.17	3.245	2.78768	5.30046
8	0	1	-1	1	17.215	8.56	3.55	2.0111	4.8493
9	0	0	0	1	17.54	6.66	2.94	2.63363	5.96599
10	-1	0	-1	1	16.345	7.115	4.58	2.29726	3.56878
11	0	0	0	1	16.792	6.4	3.59	2.62375	4.67744
12	1	0	0	0	19.475	7.53	2.544	2.58632	7.65527
13	0	0	1	-1	15.812	8.75	4.392	1.80709	3.60018
14	0	0	1	0	16.99	6.525	3.01	2.60383	5.64452
15	0	1	0	-1	17.515	11.323	4.191	1.54685	4.17919
16	1	1	0	1	18.855	7.355	2.899	2.56356	6.50397
17	1	0	0	-1	18.985	9.285	3.22	2.0447	5.89596
18	0	1	0	0	17.865	7.895	3.135	2.26282	5.69856
19	0	1	1	1	16.2	6.6	3.165	2.45455	5.11848
20	-1	1	0	1	15.295	7.935	4.875	1.92754	3.13744
21	1	0	1	1	16.873	6.34	3.192	2.66136	5.28603
22	0	0	-1	0	19.355	7.835	3.45	2.47033	5.61014
23	-1	0	0	1	15.18	7.255	4.045	2.09235	3.75278
24	1	0	-1	1	20.44	6.99	3.565	2.92418	5.73352
25	-1	-1	0	1	15.56	7.025	3.49	2.21495	4.45845
26	0	0	-1	-1	17.905	11.07	4.906	1.61743	3.64961
27	0	0	0	1	17.042	6.7	3.205	2.54358	5.31732
28	0	-1	-1	1	17.365	6.32	3.475	2.74763	4.99712
29	0	-1	0	-1	16.63	8.272	4.005	2.0104	4.15231

2.3. Conducting the experiments as per the design matrix:

The experiments were conducted using Ador submerged arc-welding equipment.

- Electrode used: Grade C (AWS-5.17-80 EH -14)
- Work piece: Mild steel plates of 200× 75×12 mm size.
- Type of joint: bead on plate.
- Fluxes: Agglomerated developed fluxes
- Electrode-to-work angle: 90◦

Twenty nine sets of bead on plates were laid down as per the design matrix by selecting trails at random. The chemical composition of base plate and electrode wire is given in Table 3.

Table 3: Chemical composition of base plate and electrode wire.

Element (%)	C	Mn	Si	S	P	Ni	Cr
Base Plate	0.23	0.4	0.13	0.04	0.06	0.07	0.11
Electrode Wire	0.07	1.9	0.1	0.03	0.02	Nil	Nil

2.4. Recording the responses and developing models from the data:

Two transverse specimens were cut from each welded plate. These specimens were prepared by the usual metallurgical polishing methods and etched with 2% nital. The profiles of the beads were traced by using optical profile projector. The response parameters namely penetration (P), reinforcement (R), width (W), weld penetration shape factor and weld reinforcement shape factor were measured. The shape relationships namely the weld penetration size factor (WPSF) which is the ratio of bead width to the height of penetration and the weld reinforcement form factor (WRFF) which is the ratio of bead width to the height of reinforcement, were calculated. The observed values of W, P, R, WPSF and WRFF are given in Table 2. The final models thus developed from the data are given below:

Bead Width (W) = + 18.28 +1.23 x A+ 0.29 x B–1.06 x C–0.10 x D + 0.20 x A^2–0.54 x B^2–0.29 x C^2–0.90 x D^2+ 0.34 x A x B – 0.60 x A x C + 0.19 x A x D + 0.29 xB x C-0.097 x B x D + 0.052 x C x D

Penetration (P) = + 6.99–0.30 x A + 0.95 x B–0.70 x C–1.53x D+0.32 x A^2+ 0.29 x B^2+0.18 x C^2+1.07x D^2–0.025x Ax B–0.20 x A x C + 0.088 x A x D-0.58 x B x C–0.48 x B x D + 0.44 x C x D

Reinforcement (R) = + 2.94-0.91x A+ 0.19 x B-0.24 x C-0.52x D + 0.40 x A^2–0.15 x B^2+0.22 x C^2 + 0.85 x D^2–0.42xAxB + 0.041xAxC + 0.41x Ax D + 0.034x B x C + 4.071E–003 x B x D + 0.012x C x D

WPSF = + 2.62 + 0.22xA–0.19 x B+0.028 x C+0.38x D–0.098 x A^2–0.16x B^2–0.100x C^2–0.35x D^2+ 0.034 x A x B–0.014 x A x C + 0.055 x A x D + 0.23x B x C + 0.062 x B x D–0.086x C x D

WRSF = + 6.27 + 1.38 x A–0.22 x B + 1.805E-003 x C + 0.52x D–0.28 x A^2 + 0.041x B^2–0.48 x C^2–1.47 x D^2 + 0.57 x A x B–0.16 x A x C–0.33 x A x D + 0.031x B x C + 0.073 x B x D + 0.019 x C x D

2.5. Checking the significance of models:

ANOVA is a statistical technique, which can infer some important conclusions based on analysis of the experimental data. The method is very useful to investigate the level of significance of influence of factor(s) or interaction of factors on a particular response. The analysis of variance (ANOVA) test was performed to evaluate the statistical significance of the fitted quadratic models and factors involved therein for response factors W, P, R, WPSF and WRFF. In addition to this, the goodness of fit of the fitted quadratic model was also evaluated through Lack of fit test. The results obtained are summarized in Tables 4-9.

Table 4: ANOVA results for Bead Width (W).

Source	Sum of Squares	DF	Mean Square	F Value	Prob > F	Remarks
Model	45.5	14	3.25	29.7	<0.0001	**significant**
A	12.8	1	12.8	117	< 0.0001	significant
B	0.73	1	0.73	6.68	0.02	significant
C	9.39	1	9.39	86	< 0.0001	significant
D	0.18	1	0.18	1.63	0.22	not significant
A^2	0.25	1	0.25	2.32	0.15	not significant
B^2	1.86	1	1.86	17	0	significant
C^2	0.56	1	0.56	5.09	0.04	significant
D^2	3.57	1	3.57	32.7	< 0.0001	significant
AB	0.46	1	0.46	4.23	0.06	not significant
AC	1.44	1	1.44	13.2	0	significant
AD	0.27	1	0.27	2.43	0.14	not significant
BC	0.34	1	0.34	3.07	0.1	not significant
BD	0.07	1	0.07	0.59	0.45	not significant
CD	0.02	1	0.02	29.7	< 0.0001	not significant
Residual	1.52	14	0.1			
Lack of Fit	0.87	10	0.08	0.54	0.8	**not significant**
Pure Error	0.64	4	0.16			

Table 5: ANOVA results for Penetration (P).

Source	Sum of Squares	DF	Mean Square	F Value	Prob > F	Remarks
Model	54.66	14	3.9	48.99	< 0.0001	**significant**
A	0.76	1	0.76	9.57	0.0079	significant
B	7.51	1	7.51	94.26	< 0.0001	significant
C	4.1	1	4.1	51.47	< 0.0001	significant
D	39.5	1	39.5	495.75	< 0.0001	significant
A^2	0.68	1	0.68	8.49	0.0113	significant
B^2	0.53	1	0.53	6.7	0.0215	significant
C^2	0.21	1	0.21	2.62	0.1276	not significant
D^2	5.1	1	5.1	64.02	< 0.0001	significant
AB	0	1	0	0.03	0.8619	not significant
AC	0.16	1	0.16	1.96	0.1835	significant
AD	0.05	1	0.05	0.68	0.4244	not significant
BC	1.34	1	1.34	16.76	0.0011	significant
BD	1.64	1	1.64	20.54	0.0005	significant
CD	1.351243	1	1.351243	16.95706	0.001	significant
Residual	1.12	14	0.08			
Lack of Fit	0.88	10	0.09	1.5	0.3692	**not significant**
Pure Error	0.23	4	0.06			

Table 6: ANOVA results for Reinforcement (R).

Source	Sum of Squares	DF	Mean Square	F Value	Prob > F	Remarks
Model	16.67	14	1.19	27.64	< 0.0001	**significant**
A	6.95	1	6.95	161.3	< 0.0001	significant
B	0.3	1	0.3	7.05	0.0188	significant
C	0.47	1	0.47	10.92	0.0052	significant
D	4.49	1	4.49	104.22	< 0.0001	significant
A^2	1.03	1	1.03	23.9	0.0002	significant
B^2	0.14	1	0.14	3.21	0.0947	not significant
C^2	0.33	1	0.33	7.57	0.0156	significant
D^2	3.17	1	3.17	73.52	< 0.0001	significant
AB	0.71	1	0.71	16.52	0.0012	significant
AC	6.56E-03	1	6.56E-03	0.15	0.7022	not significant
AD	1.19	1	1.2	27.71	0.0001	significant
BC	4.56E-03	1	4.56E-03	0.11	0.7498	not significant
BD	1.16E-04	1	1.16E-04	2.69E-03	0.9593	not significant
CD	1.02E-03	1	1.02E-03	0.024	0.8799	not significant
Residual	0.6	14	0.043			
Lack of Fit	0.38	10	0.038	0.69	0.7128	not significant
Pure Error	0.22	4	0.055			

Table 7: ANOVA results for WPSF.

Source	Sum of Squares	DF	Mean Square	F Value	Prob > F	Remarks
Model	4.02	14	0.29	29.3	< 0.0001	**significant**
A	0.42	1	0.42	42.72	< 0.0001	significant
B	0.31	1	0.31	31.64	< 0.0001	significant
C	0.01	1	0.01	0.69	0.4185	not significant
D	2.4	1	2.4	244.91	< 0.0001	significant
A^2	0.06	1	0.06	6.35	0.0245	significant
B^2	0.17	1	0.17	17.34	0.001	significant
C^2	0.06	1	0.06	6.56	0.0226	significant
D^2	0.55	1	0.55	55.77	< 0.0001	significant
AB	0	1	0	0.48	0.4988	significant
AC	0	1	0	0.09	0.7741	not significant
AD	0.02	1	0.02	2.18	0.1617	not significant
BC	0.21	1	0.21	21.31	0.0004	significant
BD	0.03	1	0.03	2.74	0.12	not significant
CD	0.05	1	0.05	5.22	0.0384	significant
Residual	0.14	14	0.01	0.14		
Lack of Fit	0.11	10	0.01	1.36	0.4123	**not significant**
Pure Error	0.03	4	0.01			

Table 8: ANOVA results for WRFF.

Source	Sum of Squares	DF	Mean Square	F Value	Prob > F	Remarks
Model	34.29	14	2.45	11.98	< 0.0001	**significant**
A	16.1	1	16.1	78.72	< 0.0001	significant
B	0.39	1	0.39	1.91	0.1886	not significant
C	0	1	0	0	0.9909	not significant
D	4.51	1	4.51	22.07	0.0003	significant
A^2	0.49	1	0.49	2.4	0.1436	not significant
B^2	0.01	1	0.01	0.05	0.8193	not significant
C^2	1.49	1	1.49	7.31	0.0171	significant
D^2	9.61	1	9.61	46.98	< 0.0001	significant
AB	1.3	1	1.3	6.34	0.0246	significant
AC	0.1	1	0.1	0.49	0.4964	not significant
AD	0.74	1	0.74	3.64	0.0772	not significant
BC	0	1	0	0.02	0.8919	not significant
BD	0.04	1	0.04	0.18	0.6754	not significant
CD	0	1	0	0.01	0.9138	not significant
Residual	2.9	14	0.2			
Lack of Fit	2	10	0.2	0.98	0.5583	**not significant**
Pure Error	0.8	4	0.2			

Table 9: Model summary statistics for Response Bead Geometry Parameters.

Bead geometry parameters	Std. Dev.	Mean	C.V. (%)	PRESS	(R^2)	Adjusted (R^2)	Predicted (R^2)	Adequate Precision (AP)
W	0.33	17	1.91	7.28	0.967	0.935	0.845	22.143
P	0.28	7.59	3.72	5.09	0.98	0.96	0.908	25.087
R	0.21	3.61	5.75	2.75	0.965	0.93	0.841	24.08
WPSF	0.099	2.34	4.24	0.71	0.967	0.934	0.829	18.614
WRFF	0.452	5.01	9.03	12.08	0.923	0.846	0.675	15.638

All the fitted models are found to be significant. Since for all the responses, the probability of F (Prob. > F) are observed to be less than 0.0001. In other words, there is only a 0.01% chance that "Model F-Value" larger than those reported in Tables 4a and 5a could occur due to noise. The values of "Prob > F" less than 0.05 observed for some factors involved in model equations, indicate that the contribution of these terms to the model is significant. On the other hand, the value of "Prob > F" greater than 0.10 indicates that the impact of model terms are not significant.

2.6. Validation of models:

To test the accuracy of the models in actual applications, conformity test runs were conducted by assigning different values for process variables within their working limits. Specimens were cut from the conformity test plates and their bead profiles were traced. All bead dimensions were measured. The percentage of errors, which give the deviation of predicted results of responses from the actual measured values, were also calculated and presented in Table 10. It is found from the table that the average error for all models is less than 3%.

Table 10: Comparison of actual and predicted values of weld bead parameters.

S. No.	Process variables in coded form				Predicted values of bead parameters			Actual values of bead parameters			% Error		
	A	B	C	D	W	P	R	W	P	R	W	P	R
1	1	-1	0	1	17.83	6.48	3.24	17.29	6.54	3.3	-3.02	1	1.85
2	0	0	0	1	17.28	6.53	3.27	17.63	6.51	3.19	2.02	-0.003	-2.44
3	-1	0	-1	1	16.17	7.3	4.66	16.63	7.12	4.62	2.87	-2.46	-3
4	1	1	0	1	18.89	7.37	2.79	18.87	7.39	2.82	-0.1	0.27	1.07
5	0	-1	0	0	17.45	6.33	2.6	17.57	6.51	2.67	0.68	2.84	2.69
6	0	1	0	0	18.03	8.23	2.98	18.12	7.99	3.06	0.49	-2.91	3

3. Analysis of results and discussion:

The mathematical models developed above can be employed to predict the geometry of weld bead and shape relationships for the range of parameters used in the investigation by substituting their respective values in coded form. Based on these models, the main and the interaction effects of the process parameters on the bead geometry were computed and plotted as depicted in Figs. 1-13. The results show the general trends between the cause and effect.

3.1. Direct effects of process variables on bead geometry:

Fig.1 shows effect of process parameters on bead width. It is apparent that bead width increases with for all values of open circuit voltage. As shown in Fig. 1 bead width (W) increases from 17.24 to 19.70 mm with the increase in open circuit voltage from 32 to 38 volts. It can be attributed to the increase in arc length with the increase in open circuit voltage, which in turn results in spreading of the arc cone at its base which results in more melting of work piece instead of penetrating the plate. This extension in bead width causes corresponding reduction in penetration and reinforcement. In fact excessive increase in voltage can result in nearly flat bead. Bead width increases from 17.44 to 18.03 mm with increase in welding current from 375 to 475 amperes. This effect is due to increase in heat input and the weight of the weld metal deposited [13]. These factors contribute to increase in weld pool size and consequently increase the bead width. As shown in Fig.1, Weld bead width decreases steadily with the increase in welding speed. The bead width decreases from 19.04 to 16.92 with increase in welding speed from 24 to 30 m/hr. This negative effect of speed on W is due to the fact that when speed increases, the thermal energy transmitted to the base plate from the arc or line power per unit length of the weld bead decreases and less filler metal is deposited per unit length of weld bead, resulting in thinner and narrower weld bead. Hence, at lower travel speeds, the weld bead is larger in mass, whereas at higher travel speeds, it is lesser in mass. If speed decreases, the bead becomes wider, flatter and smoother [14]. It can be explained on the basis of decrease in metal deposited rate and heat input with the increase in welding speed. The bead width increases from 17.44 to 18.04 mm with change in current from 375 to 475 amperes. The combined effect of these factors results in decrease in bead width with the increase in welding speed. The effect of basicity index on bead width is not significant.

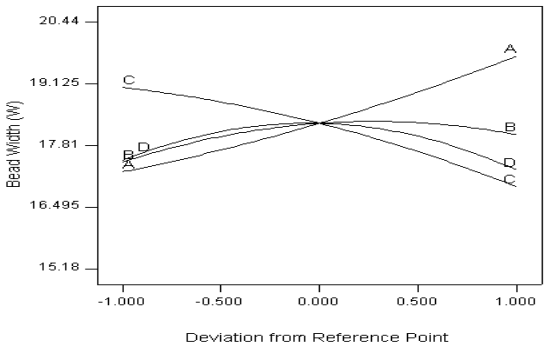

Figure 1: Effect of process parameters on bead width.

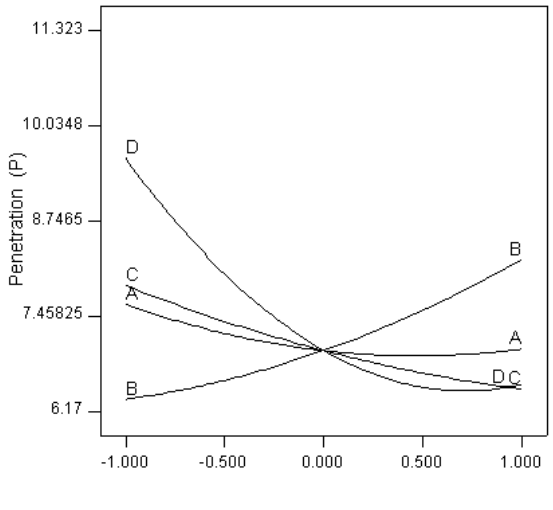

Figure 2: Effect of process parameters on Penetration.

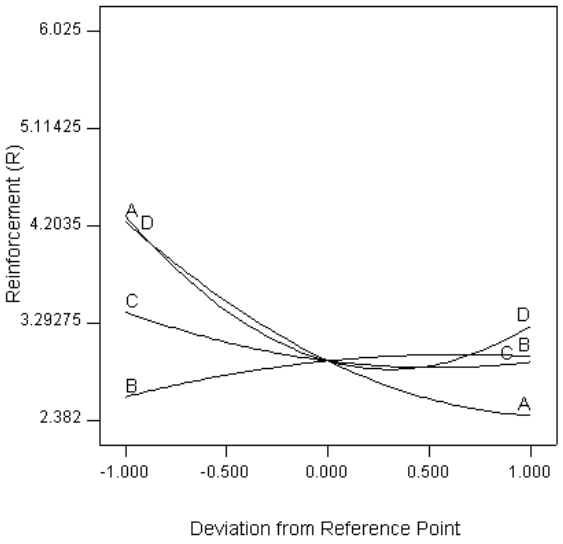

Figure 3: Effect of process parameters on Reinforcement.

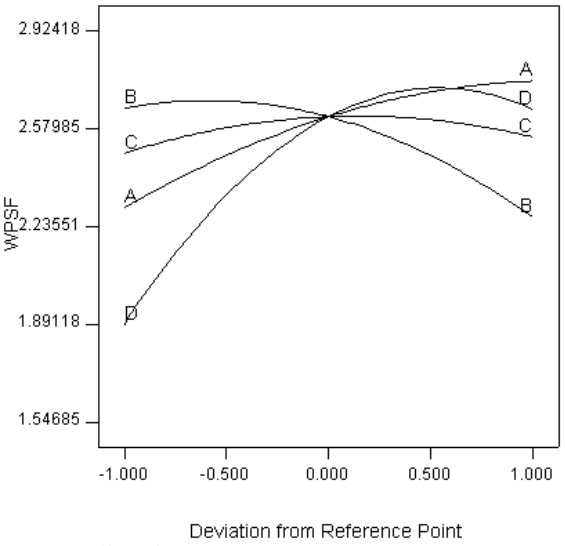

Figure 4: Effect of process parameters on WPSF.

As shown in Fig.2, the penetration (P) increases from 6.33 to 8.22 mm with the increase in welding current from 375 to 475 amperes. Increase in current gives rise to enhanced line power per unit length of the weld bead and higher current density, causing larger volume of the base material to melt and hence, deeper penetration. As current increases the temperature and hence the heat content of the droplets increases, which results in more heat being transferred to the base material. Increase in current also increases momentum of the droplets, which on striking the weld pool causes a deeper penetration. An increase in welding current, with other variables remaining constant, results in increased depth of penetration and weld width, increased deposition rate and increased weld bead size and shape at a given cross-section. It is also attributed to the increase in digging power of the arc with the increase in welding current. As the current increases, the intensity of the arc and hence the digging power of the arc and penetration increases. As depicted in Fig.3, the penetration decreases from 7.86 to 6.47 mm with the increase in welding speed from 24 to 30 m/hr. This could obviously be due to the reduced line power per unit length of weld bead as speed increases. Also, at higher welding speeds, the electrode travels faster and covers more distance per unit time. The combined effects of lesser line power and faster electrode travel speed results in decreased metal deposition rate per unit length of weld bead [12]. It is also attributed to decrease in heat input, metal deposition rate and digging power of the arc with the increase in welding speed resulting in decrease in weld metal penetration. From Fig.3, P decreases from 7.61 to 7.01 when open circuit voltage increases from 32 to 38 volts. This is obviously due to the fact that the increase in voltage results in increased arc length and spreading of arc cone at its base which results in more melting of work piece surface instead of penetrating the plate. In fact, excessive increase in voltage can result in nearly flat bead. Flux basicity also influences the penetration. It is observed from Fig.3, the higher value of penetration i.e 9.59 mm is obtained with using low basicity index flux (0.7), because low basicity index fluxes have high viscosity which enhances the tendency of heat concentration in the narrow zone and hence high penetration. This is consistent with the study conducted by Gupta [15].

From Fig. 3 it is observed that the reinforcement (R) decreases with the increase in open circuit voltage and welding speed and increase with the increase in welding current. Reinforcement decreases with increase in basicity index due to similar reasons as described for penetration. It is seen from this graph that reinforcement decreases from 4.24 to 2.42 mm with change of voltage from 32 to 38 volts, and decreases from 3.39 to 2.92 mm when welding speed increases from 24 to 30 m/hr. When current changes from 375 to 475 amperes, it changes from 2.59 to 2.97 mm. Its value increases from 4.29 to 3.26 mm with increase in basicity index from 0.6 to 1.2.The reasons for these changes are due to same reasons as described in preceding section for penetration.

Fig.4 and Fig. 5 shows Weld penetration shape factor (WPSF) increases from 2.37 to 2.67 and with the increase in open circuit voltage from 32 to 38 volts and weld reinforcement form factor WRFF increases from 4.78 to 7.02 with increase of open circuit voltage from 32 to 38 volts. This positive effect of voltage on both the factors is due to the following reasons. Bead width (W) increases almost steadily but P and R decrease little as voltage increases from −1 to +1 limit as discussed already. Hence,

they increase steadily as voltage increases. WPSF decreases when current increases, but it remains nearly constant from 375 to 400 amperes and it decreases from 2.61 to 2.44 (Fig.5) when current changes from 375 to 475 amperes. This could be due to reason that WPSF which is the ratio of W/P, decreases when current changes from 400 ampere to 475 amperes, because rate of increase of P is more than that of W with in this range of current. It is also observed in Fig.5 that WPSF increases 1.82 to 2.42 with increase of basicity index from 0.6 to 1.2. It is seen from Fig.6 that WRFF decreases from 4.05 to 5.23 with increase of basicity index from 0.6 to 1.2. These results can be explained with the help of effects of welding variables on weld width, penetration and reinforcement respectively.

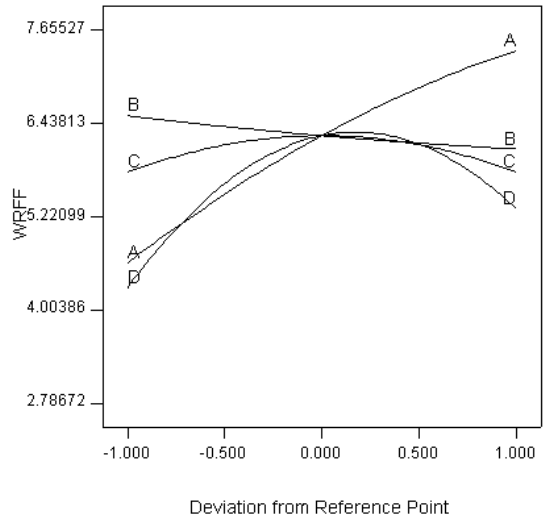

Figure 5: Effect of process parameters on WRFF.

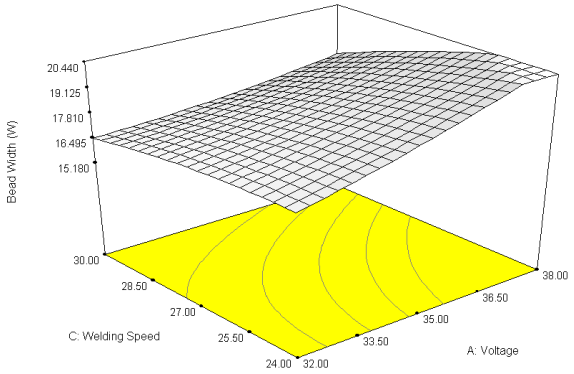

Figure 6: Interaction effect of voltage and speed on bead width.

3.2. Interaction effects of process variables on bead geometry:

3.2.1. Interaction effects on bead width (W) and penetration (P):

It is apparent from Fig. 6 showing interaction of open circuit voltage and welding speed on W that the increase in voltage increases W for all values of speed. The bead width increases from 17.40 to 21.07 mm and from 16.49 to 17.75 mm with the increase in voltage from 32 to 38 volts, at the welding speed 24 and 30 m/hr respectively. It shows that the increasing trend of bead width with the increase in open circuit voltage decreases with the increase in welding speed. It is due to the fact that open circuit voltage has a positive effect whereas welding speed has negative effect on bead width. Therefore the combined effect of these parameters causes the decrease in increasing trend of bead width with the increase in open circuit voltage.

From the response surface plot in Fig.7, it is evident that P increases with the increase in welding current for all values of welding speed. It shows that the weld metal penetration increases from 6.63 to 9.67 mm and from 6.38 to 7.12, with increase in current, at the welding speed of 24 to 30 m/hr respectively. The rate of increase in P with the increase in current decreases gradually as speed increases. These effects on P are due to the reasons that current has positive effect but speed has a negative effect on P as discussed already in the direct effects of current and speed on P. It is found that at lower values of speed, the positive effect of current on P is stronger but at higher values of speed, the negative effect of speed on P is stronger. This is also consistent with the findings of Rayes [16]. From the contour surface, it is noted that P is maximum (about 9.67 mm) when current and speed are at their maximum (+1) and minimum (−1) limits, respectively, and the lowest value of P (about 6.004 mm) is obtained when current and speed are at their minimum and maximum limits, respectively. From Fig.8 it is observed that penetration increases from 8.45 to 11.31 mm and from 6.38 to 7.28, with increase in current, at the basicity index of 0.6 and 1.2 respectively. It is evident form Fig.10 that penetration decreases form10.91 to 8.63 and from 6.97 to 6.45 with increase in welding speed from low basicity index to its higher value. These results can be explained with the help of effects of welding variables such as welding speed and basicity index penetration.

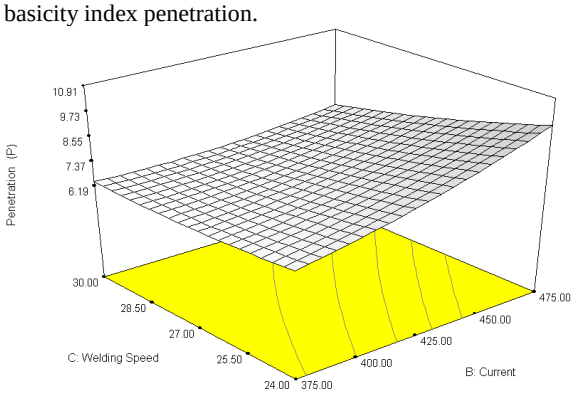

Figure 7: Interaction effect of current and speed on penetration.

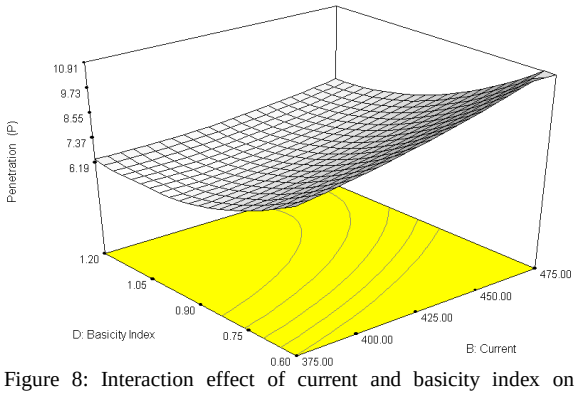

Figure 8: Interaction effect of current and basicity index on penetration.

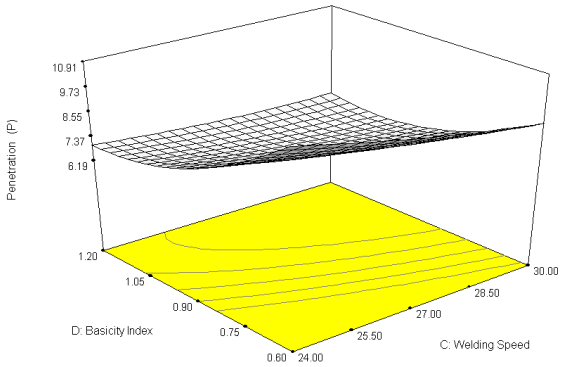

Figure 9: Interaction effect of speed and on basicity index on Penetration.

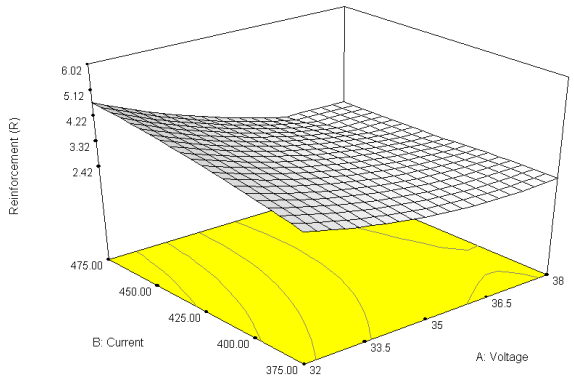

Figure 10: Interaction effect of voltage and current on Reinforcement.

3.2.2. Interaction effects on reinforcement (R), WPRF and WPSF:

It is observed in Fig.10 and 11 that reinforcement decreases with the increase in voltage, when the current changes from 375 to 475 amperes and it also decreases with voltage from low basicity index to its higher value. These interaction effects can be explained on the basis of effect of voltage, current and basicity index on reinforcement. Voltage has positive effect on reinforcement whereas current has negative effect on reinforcement. The negative effect is dominant while considering the interaction of voltage and current. Reinforcement decreases with increase in voltage from 32 to 38 volts, for all values of current.

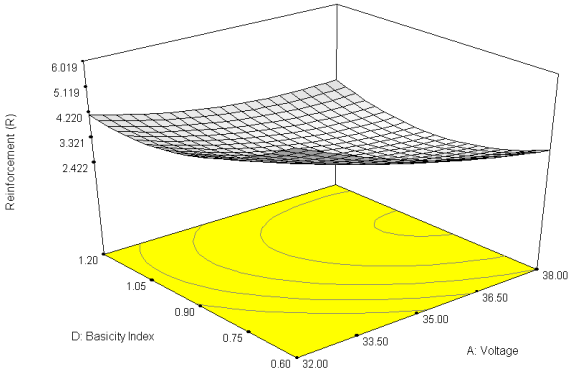

Figure 11: Interaction effect of voltage and basicity index on reinforcement.

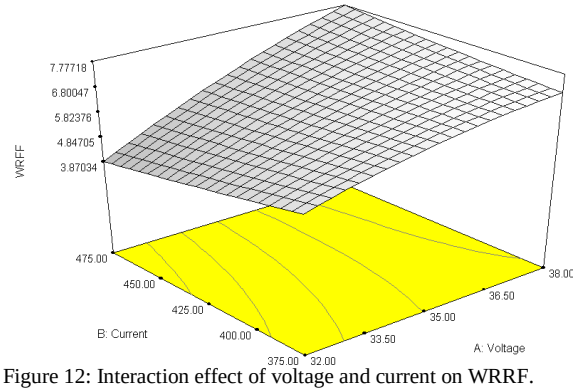

Figure 12: Interaction effect of voltage and current on WRRF.

Fig.12 shows the interaction effect of voltage and current on WRFF. It is evident from these graphs that WRFF increases for all values of current when voltage increases from 32 to 38 volts. But the increasing trend of WRFF in more at higher value of current i.e. at 475 amperes that that at 375 amperes. This is due to fact that WRFF= W/R, W increases with increase of voltage and nearly remains constant with change of current whereas R decreases with increasing voltage and increases with increase of current [17]. Thus voltage has positive effect on WRFF whereas current has negative effect on WRFF. This increasing trend of WRFF at higher current is due to more positive effect of voltage on WRFF. This can also be explained on the basis of effects of voltage and current on bead width and reinforcement. The interaction effects of welding speed and basicity index on WPSF can also be explained due to the effect of welding speed and basicity index on bead width and penetration (Fig. 13).

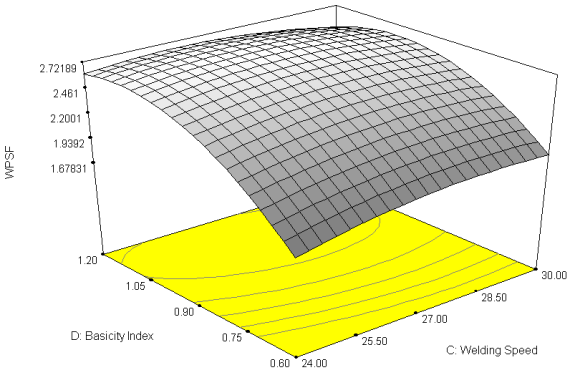

Figure 13: Interaction effect of Speed and basicity on WPSF.

4. Conclusion

In the present study, detailed experimentation and analyses have been carried out in order to emphasize the extent of utilizing developed flux prepared from waste flux dust in the conventional SAW, on different bead geometry parameters like: weld penetration shape factor, weld reinforcement form factor, bead width, penetration and reinforcement. The important parameters, which significantly affect these bead quality characteristics, have also been identified by ANOVA technique. Within limitations of the present work, the following conclusions are summarized as follows:

- Response surface methodology Box-Behnken Design (BBD) can be employed easily for developing mathematical models for predicting important weld

bead dimensions and shape relationships within the optimal range of process control variables for SAW.

- The models developed can be employed easily in automated or robotic welding in the form of a program, for obtaining the desired weld bead dimensions.
- Out of the four process variables considered, welding current had a significant positive effect but welding speed had an appreciable negative effect on most of the important bead parameters. Penetration (P) increased by 2 mm with the increase in welding current from 375 to 475 amperes whereas penetration decreased by about 1.4 mm with the increase in welding speed from 24 to 30 m/hr. The bead width decreased by 2.12 mm with increase in welding speed from 24 to 30 m/hr. Reinforcement decreased from 3.39 to 2.92 mm when welding speed increases from 24 to 30 m/hr, but when current changed from 375 to 475 amperes, it value increased from 2.59 to 2.97 mm.
- Open circuit voltage had a negative effect on penetration, but more significant negative effect was observed on reinforcement. Voltage had a significant positive effect on bead width, weld penetration size factor and weld reinforcement form factor.
- The interaction of welding current and speed had an appreciable effect on penetration and penetration size factor, but this interaction had not any significant effect on bead width and reinforcement form factor. Penetration increased with the increase in current for all values of welding speed but this increasing rate of the penetration with the increase in B gradually decreased with the increase in C.
- The interaction of voltage and current had significant effect on reinforcement and weld reinforcement form factor effect as compared to its effect on other response parameters. Reinforcement decreased with the increase in voltage for all values of current whereas WRFF increased with voltage for all current values. Positive effect of voltage was more dominant in WRFF as compared to negative effect of current for the trends in case of WRFF, whereas reverse is the case for reinforcement. This increasing trend of WRFF at higher current was due to more positive effect of voltage on WRFF.

Thus it is seen that with in the present experimental domain, using the developed flux prepared from waste flux dust had no adverse effect on bead geometry. Detailed experimentation on the effect of developed flux on mechanical properties and metallurgical characteristics of the weldment to be rigorously done. If the outcomes becomes positive, then developed flux prepared this way can be recommended to use as an alternative to fresh flux in practical situations to yield 'waste to wealth'.

Acknowledgment

The authors wish to thank Thapar University, Patiala and Punjab Engineering College Chandigarh for providing the facilities for carrying out the experiments in undertaking this work.

References

[1] Parmer R S. Welding Processes and Technology. New Delhi: Khanna Publishers; 1992.
[2] Hould croft PT. Submerged Arc Welding. second ed., Cambridge, England: Abington Publishing; 1989.
[3] Brien RL. Welding Handbook. vol.2, 8th edition, Miami, U.S.A: American Welding society; 1978.
[4] Vinod. K, N. Mohan , J.S. Khamba, "Development of cost effective agglomerated fluxes from waste flux dust for submerged arc welding" . Proceedings of World Congress on Engineering, , Imperial College, London, 2009.
[5] N. Murugan, R.S. Parmer, S.K. Sud, "Effect of submerged arc process variables on dilution and bead geometry in single wire surfacing". J. Mater. Process. Technol, Vol.37, 1993, 767–780.
[6] V.K. Gupta, R.S. Parmer, "Fractional factorial technique to predict dimensions of the weld bead in automatic submerged arc welding". J. Inst. Eng. (India), Vol. 70, 1989, 67-86.
[7] Myers R, Montgomery D. Response surface methodology. New York: John Wiley & Sons; 2004.
[8] S. Datta, A. Bandyopadhyay, P.K. Pal , "Quadratic response surface modeling for prediction of bead geometry in submerged arc welding". Indian Weld J, Vol. 38, No.4, 2006, 33–43
[9] S. Datta, M. Sundar, A. Bandyopadhyay, P.K. Pal, G. Nandi, S.C. Roy, "Statistical modeling for predicting bead volume of submerged arc butt welds". Australas Weld J, Vol. 51(2), 2006, 39–47.
[10] Horng. Jenn. Tsong, Liu. Nun. Ming, Ko. Ta. Chiang. "Investigating the machinability of hardfield steel in hard turning with Al2O3/TiC mixed ceramic tool based on response surface methodology". J. Mater. Process. Technol, Vol. 208, 2008, 532–541.
[11] G.E.P. Box, D.W. Behnken, "Some new three level designs for the study of quantitative variables". Techno metrics, Vol.2, 1960, 455-475.
[12] Box GEP, Hunter WG, Hunter JS. Statistics for experimenters: an introduction to design, data analysis, and model building. New York: John Wiley & Sons; 1976.
[13] V. Gunuraj, N. Murgun, "Application of response surface methodology for predicting weld bead quality in submerged arc welding of pipes". Journal of material processing technology, Vol.88, 1999, 266-275.
[14] Olson D L, Dixon R, Liby AL. Welding Theory and Practice. North-Holland Publication; 1990.
[15] S.R. Gupta, P.C. Gupta, "Investigate into flux consumption in submerged arc welding". Indian welding journal, Vol. 21, No. 3, 1988, 365-369.
[16] M. El. Rayes, "The influence of various hybrid welding parameters on bead geometry". Welding Journal, Vol. 85, No.5, 2004, 147s-155s.
[17] S. Datta, A. Bandhopadhayaay, P.K. Pal, "Modeling and optimization of features of bead geometry including percentage dilution in submerged arc welding using mixture of fresh and fused flux". International Journal of advanced Manufacturing Technology, Vol. 36, No.11, 2008, 1080-1090.

Appendix

Notations

P: Penetration
RSM: Response surface methodology
R: Reinforcement
W: Bead width
WPSF: Weld penetration size factor
WRFF: Weld reinforcement form factor